Mechanistic Analysis Reveals Key Role of Interchalcogen Multicatalysis in Photo-Aerobic 3-Pyrroline Syntheses by Aza-Wacker Cyclizations

Sebastian Graf+,[a] Henner Pesch+,[b] Theresa Appleson,[a] Tao Lei,[a] Alexander Breder,*[a] and Inke Siewert*[b]

A light-driven dual and ternary catalytic aza-Wacker protocol for the construction of 3-pyrrolines by partially disulfide-assisted selenium-π-acid multicatalysis is reported. A structurally diverse array of sulfonamides possessing homopolar mono-, di- and trisubstituted olefinic double bonds is selectively converted to the corresponding 3-pyrrolines in up to 95% isolated yield and with good functional group tolerance. Advanced electrochemical mechanistic investigations of the protocol suggest a dual role of the disulfide co-catalyst. On the one hand, the disulfide serves as an electron hole shuttle between the excited photo-redox catalyst and the selenium co-catalyst. On the other hand, the sulfur species engages in the final, product releasing step of the catalytic cycle by accelerating the β-elimination of the selenium moiety, which was found in many cases to lead to considerably improved product yields.

Introduction

N-Heterocycles constitute a highly relevant compound class, which is amply found both in biological and industrial contexts, for instance, as pharmaceuticals, crop protecting agents, and secondary metabolites (Scheme 1a).[1] Already in 2010, about 59% of all FDA approved small-molecule drugs contained *N*-heterocycles, out of which five- and six-membered rings represented the most frequently encountered skeletal patterns.[1c] Considering the economic and scientific gravitas of azacycles, it is not surprising that this compound class has been subject of intensive method-oriented research over the last decades.[2,3] A particularly prominent catalytic avenue toward non-aromatic *N*-heterocycles is the intramolecular aza-Wacker reaction, which was successfully implemented in the wide-scale manufacture of pyrrolidines, piperidines, and azepanes.[2–4] Notably, cognate procedures for the catalytic synthesis of substituted 3-pyrrolines have remained elusive so far.[5] Instead, other techniques such as Lewis-acid or transition metal-catalyzed allylic substitutions of alkenes with pre-installed
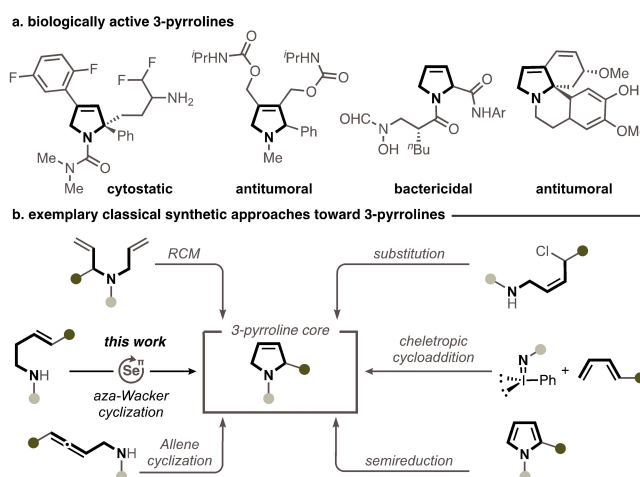
Scheme 1. [a] 3-Pyrrolines as core motifs of biologically active natural and anthropogenic compounds. [b] Exemplary synthetic routes toward 3-pyrrolines including a heretofore unprecedented selenium-π-acid catalyzed 5-*endo*-trig aza-Wacker cyclization.

nucleofuges,[6] ring-closing alkene metathesis,[6d,7] [3+2]- and cheletropic cycloadditions,[6d,8] hydroaminations,[6d,9] or stoichio-metric iodocyclizations of unsaturated sulfonamides[10] were established (Scheme 1b). Despite the great success that has been accomplished with each of these methods, they often require pre-activated building blocks and/or entail the generation of carbon-containing waste products. In contrast, the aza-Wacker reaction not only allows for the use of non-activated alkenes as precursors but also, depending on the conditions, enables the use of ambient air[4,11] or electricity[12,13] as sustainable oxidants, which significantly increases the carbon efficiency while reducing the production of waste.[14] Considering the expediency, resource efficiency and atom-economy,[15] the implementation of catalytic, photo-aerobic or anodic aza-

[a] S. Graf,+ T. Appleson, Dr. T. Lei, Prof. Dr. A. Breder
     Universität Regensburg, Institut für Organische Chemie,
     Universitätstrasse 31, 93053 Regensburg, Germany
     E-mail: alexander.breder@ur.de

[b] H. Pesch,+ Prof. Dr. I. Siewert
     Universität Göttingen, Institut für Anorganische Chemie
     Tammannstrasse 4, 37077 Göttingen, Germany
     E-mail: inke.siewert@chemie.uni-goettingen.de

[+] S.G. and H.P. contributed equally to this study.

Supporting information for this article is available on the WWW under https://doi.org/10.1002/cssc.202301518

ChemSusChem

Research Article
doi.org/10.1002/cssc.202301518

Chemistry Europe
European Chemical
Societies Publishing

Wacker manifolds into the synthesis of 3-pyrrolines would therefore be highly desirable.

So far, aza-Wacker reactions are dominantly executed with transition metal catalysts such as Pd.[16] From a mechanistic viewpoint, these reactions often entail specific restrictions, which manifest in the observed product selectivity. More concretely, upon β-hydride elimination in the final step, the olefinic double bond is preferentially restored in a terminal position, in conjugation to a pre-existing π-system, or exocyclic in the case of small and medium-sized azacycles (up to six ring members).[11] This circumstance has hitherto prevented the aza-Wacker cyclization from being applied in the synthesis of 3-pyrrolines from linear precursors. On the contrary, selenium-π-acids[17] were recently introduced as mechanistically complementary catalysts for aza-Wacker reactions, which do not exhibit the aforesaid selectivity restrictions.[13,18] The reason for this deviant behavior is the lacking propensity of selenium to undergo reversible β-hydride elimination and, consequently, product isomerization. Therefore, selenium-π-acids have been successfully applied in various selective inter- and intramolecular allylic and vinylic alkene aminations,[13,18] which were, in part, unamenable to Pd or Cu catalysis. Despite this progress, however, the 3-pyrroline motif had remained an elusive target within the realm of selenium-π-acid catalysis. Based on previous investigations in our laboratories on photo-aerobic[19] and anodic[13] selenium-π-acid-catalyzed 5-endo-trig lactonizations of enoic acids, we surmised that this kind of methodology might become suitable for the synthesis of 3-pyrrolines from unsaturated amine derivatives by way of a formal 5-endo-trig aza-Wacker cyclization (Scheme 1b).
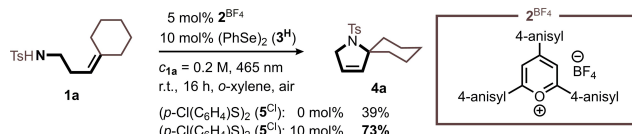
Now, we report herein a versatile protocol for the synthesis of 3-pyrrolines from linear, homoallylic sulfonamides through the ternary merger of selenium-π-acid-, disulfide-, and aerobic photoredox catalysis. Mechanistic investigations conducted by electrochemical methods indicate an unprecedented interchalcogen mechanism, in which the oxidized sulfide-species does not only act as an electron hole shuttle but is also engaged in the product-releasing elimination step.

Results and Discussion

In preliminary experiments on the 5- and 6-exo-trig aza-Wacker cyclization of N-alkenylated p-toluenesulfonamides **1** we realized that optimal substrate conversion was achieved with 5 mol% of 2,4,6-tris(4-methoxyphenyl)pyrylium tetrafluoroborate (2^{BF4}) and 10 mol% diphenyldiselenide (3^H) at 465 nm irradiation under ambient air in o-xylene (SI, Table S5). The investigations included solvent screening from polar to nonpolar solvents and variations in the concentration of the reagents and co-catalysts. Interestingly, more polar solvents consistently led to lower yields, which is in stark contrast to previous observations in our laboratories.[19] The reason for that is that 2^{BF4} is poorly soluble in nonpolar solvents, thus, use of such media typically led – if at all – to significantly diminished yields due to a very low steady state concentration of the excited state photoredox catalyst.

The abovementioned conditions were used as a starting point to develop the aspired selenium-π-acid-catalyzed 3-pyrroline synthesis. At the outset, tertiary alkene **1a** was chosen as the test substrate to obviate the risk of forming an undesired 2-pyrroline derivative (Scheme 2a). Gratifyingly, targeted 3-pyrroline **4a** was formed in 39% crude yield in o-xylene at ambient temperature using the abovementioned catalyst combination. In a parallel study on selenium-π-acid-catalyzed photo-aerobic lactonizations of enoic acids we found that certain sulfur species such as disulfides can have a rate-enhancing effect,[20] which prompted us to test (4-Cl(C_6H_4)S)$_2$ (5^{Cl}, 10 mol%) as a co-catalyst in the conversion of alkene **1a**. Under these modified conditions, product **4a** was obtained in a significantly increased yield of 73% (Scheme 2a). Finally, we analyzed the regioselectivity of the dual (i.e., without 5^{Cl}) and the ternary catalyst system (i.e., with 5^{Cl}) using a substrate that principally allows the formation of both the 2- and 3-pyrroline isomer (Scheme 2b). For this purpose, tertiary alkene **1b** was converted under dual and ternary catalytic conditions, which furnished in either case solely the Hofmann elimination products **4b** with a crude ratio of 3.3:1 and 3.7:1 ratio, respectively, in preference for the 3-pyrroline regioisomer (Scheme 2b). Since the restora-
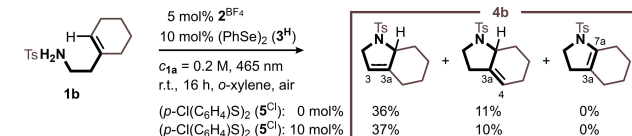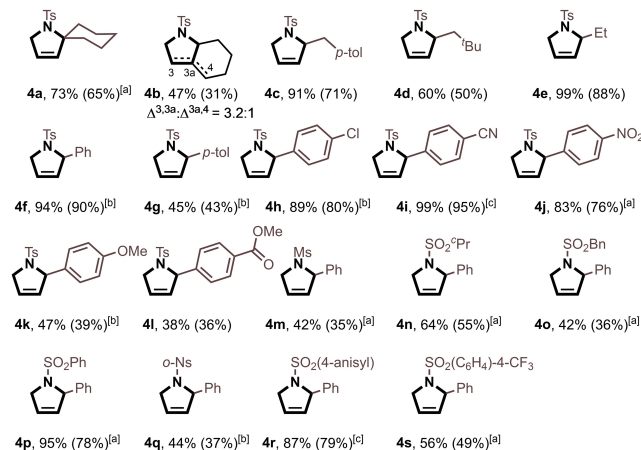

Scheme 2. Standard reaction conditions: **1** (0.5 mmol) in o-xylene ($c_1 = 0.2$ M), 3^H (10 mol%) and 2^{BF4} (5 mol%) at 465 nm and 19 °C to 23 °C, irradiation for 4 h to 48 h. Deviations from standard conditions: [a] Addition of 5^{Cl} (10 mol%). [b] 3^H (2 x 10 mol% at $t_1 = 0$ h and $t_2 = 12$-16 h) and 2^{BF4} (2 x 5 mol% at $t_1 = 0$ h and $t_2 = 12$-16 h). [c] Addition of 5^{Cl} (10 mol%) and 2-nitrobenzaldehyde (25 mol%). Yields in parentheses refer to isolated products. Isomeric ratio depicted for **4b** was determined from the purified product.

ChemSusChem

Research Article
doi.org/10.1002/cssc.202301518

Chemistry
Europe

European Chemical
Societies Publishing

tion of the alkene moiety in products **4b** selectively occurs toward positions 3 and 4 (i.e., Hofmann selectivity, Scheme 2b), we concluded that the final step may proceed through a sterically controlled E2 elimination pathway, and that 3-pyrroline formation might consequently be the generally preferred outcome for this kind of aza-Wacker cyclization.

The above-stated conjecture turned out to be true, as we realized when a variety of substrates **1c-s** was subjected to our reaction conditions (Scheme 2c). In all cases tested, 3-pyrroline formation was dominant, irrespective of the electronic nature of the residues at position 2 (i.e., electron withdrawing or donating functionalities; cf. examples **4h-j** vs. **4g/k**). During these studies we also found out that substrates with sterically less demanding groups at the distal position of the alkene moiety (i.e., **1c-e**, Scheme 2c) reacted already in reasonable to good yields without disulfide co-catalyst **5^Cl**. For most of the remaining substrates, however, we either used co-catalyst **5^Cl** (conditions a and c) or sequentially added selenium catalyst **3^H** and **2^BF4** in two portions (condition b) to reach good conversions. This reaction behavior prompted us to investigate the impact of **5^Cl** and of the solvent in more detail. Therefore, we turned to electrochemical methods as these proved to be valuable tools for the mechanistic analysis of such redox catalysis.[13]

At first, we conducted bulk electrolysis experiments under various conditions in order to confirm that oxidation under electrochemical and photochemical conditions lead to the same products. Diselenide **3^OMe** was chosen under electrochemical conditions, as it exhibits a lower oxidation potential than **3^H** in MeCN[13] and thus allows to run the reaction under milder conditions. We started with controlled current electrolysis (CCE) experiments in fluorobenzene as non-polar solvent ($\varepsilon_r = 5.42$ F/m), because the photoredox catalytic protocol exhibited higher yields in such solvents.[20] CCE experiments of alkene **1f** in the presence of 10 mol% of the diselenide catalyst **3^OMe** furnished product **4f** in yields of 35% at full conversion (Table 1, entry 1). Notably, in contrast to the photochemical protocol, addition of the disulfide **5^Cl** had virtually no effect on the yield (entry 2). Additionally, the yield was higher in MeCN as

a polar solvent ($\varepsilon = 37.5$ F/m) than in less polar fluorobenzene, affording **4f** in 55% yield (entry 3). The catalyst loading could be lowered down to 2.5 mol-% without significant loss in yield and conversion (up to 49%, entries 4 and 5). These results show that the electrochemical aza-Wacker reaction leads to the same product as under photochemical conditions, though distinct differences on the effect of the solvent and the additive **5^Cl** were observed.

From previous investigations[13] we knew that diselenide catalysts operate through a sequence of electrophilic addition and elimination steps.[13,18] Therefore, we hypothesized that a similar two-step process might also be operative in this aza-Wacker reaction, that is, an electrophilic addition of the oxidized diselenide **3** at the alkene furnishes the selane intermediate **6**, which is followed by an oxidatively induced elimination forming the 3-pyrroline **4** (Scheme 3). We focused on the model reaction of alkene **1f** with **3^OMe** and **3^H** for the mechanistic studies.

The CV (cyclic voltammetry) data of the diselenide **3^OMe** showed one irreversible oxidation at a peak potential of $E_p = 0.82$ V in MeCN and of $E_p = 0.74$ V vs. Fc$^{+|0}$ in fluorobenzene ($v = 0.2$ Vs^{-1}, Fc = ferrocene), which shift with increasing scan rates and remain irreversible in both solvents up to a scan rate of 2 Vs^{-1} (Figure 1, Figure S5, if not otherwise stated, all potentials are given vs. the Fc$^{+|0}$ redox couple). CV measurements of diselenide **3^H** revealed slightly higher oxidation potentials ($E_p = 0.98$ V in MeCN[13] and $E_p = 0.96$ V in fluorobenzene, $v = 0.2$ Vs^{-1}) than those of analog **3^OMe** in the respective solvents due to the electron-donating character of the methoxy groups (Figure S2). The irreversible oxidation of **3^OMe** in both solvents points to a fast follow-up chemical reaction upon oxidation, as was observed previously for **3^H** in MeCN.[13] The oxidation processes of **3^OMe** and **3^H[13]** are one electron oxidations as determined from the scan rate dependent measurements using the Randles-Ševčík equation (Figure S3, S6).

Table 1. Results of the electrolysis experiments.

entry	3^{OMe} [mol%]	solvent	additive	yield [%]
1[a]	10	PhF	–	35
2[a]	10	PhF	5^{Cl}	33
3[b]	10	MeCN	–	55
4[b]	5	MeCN	–	45
5[b]	2.5	MeCN	–	49

Conducting salt = ^{n}Bu$_4$NPF$_6$ ($c = 0.1$ M) in MeCN and ^{n}Bu$_4$NB(C$_6$F$_5$)$_4$ ($c = 0.1$ M) in fluorobenzene. Yields were determined by ^{1}H-NMR spectroscopy using 1,3,5-trimethoxybenzene as an internal standard. [a] Reactions performed under constant current of 400 μA. [b] Reactions performed under constant potential of 1.15 V vs. Ag$^{+|0}$ ($c_{AgNO3} = 0.01$ M MeCN).
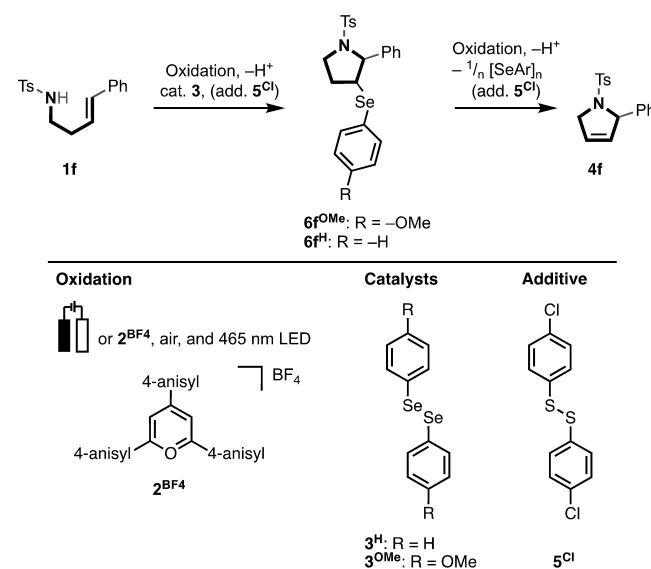
Scheme 3. Initial mechanistic model proposed for the photo- and electrochemically driven aza-Wacker-type cyclization.
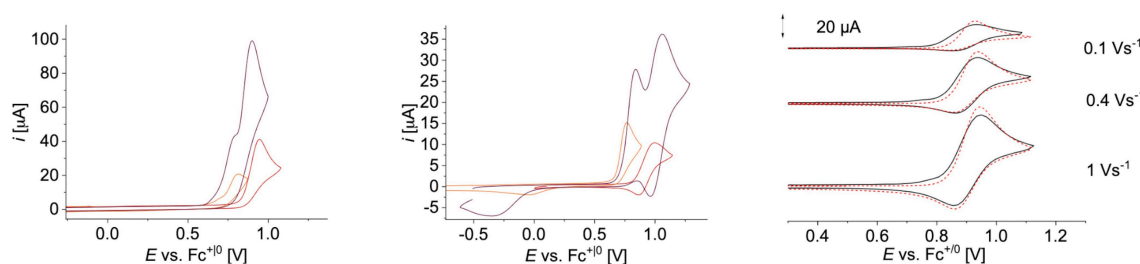
ChemSusChem

Research Article
doi.org/10.1002/cssc.202301518

Chemistry Europe
European Chemical
Societies Publishing

Figure 1. CV measurements of 3^{OMe} (orange), 3^{OMe} and $1f$ (dark brown), and $6f^{OMe}$ (red) in MeCN (left), 0.1 M $^nBu_4NPF_6$, and fluorobenzene (middle), 0.1 M $^nBu_4NB(C_6F_5)_4$, $\nu = 0.2$ Vs^{-1}. Right: measured (solid line) and simulated (dashed line) CV data of $6f^{OMe}$ in fluorobenzene. Simulation parameters $E^0 = 0.905$ V, $\alpha = 0.5$, $k_s = 0.05$ cm·s^{-1}, $D = 1.7 \times 10^{-5}$ cm^2 s^{-1}, $k_{chem} = 2.2 \times 10^3$ M^{-1}·s^{-1}.

Upon addition of 5 equiv. of the substrate $1f$ to a solution of 3^{OMe} and 3^H in MeCN, a second irreversible oxidation peak appeared in the CV data at $E_p = 0.90$ V and 1.14 V ($\nu = 0.2$ Vs^{-1}), respectively. The new oxidation peaks shift with increasing scan rates and remain irreversible up to $\nu = 2$ Vs^{-1}, indicating again a fast follow up reaction after oxidation (Figure 1, Figure S4, S7). These new features belong to the oxidations of the selane intermediates $6f^{OMe}$ and $6f^H$, respectively, as confirmed by independent syntheses of the compounds and their electrochemical investigation. The CV data of $6f^{OMe}$ and $6f^H$ show the same redox behaviors with irreversible oxidation processes at the respective potentials (Figure 1, Figure S9, S11). These observations confirm our initial hypothesis that the oxidation of the catalyst $3^{OMe/H}$ is followed by a fast chemical reaction with the substrate generating the intermediate $6f^{OMe/H}$. Notably, we do not observe a current increase in the CV experiment as would be indicative for a catalytic reaction, that is, we only reach one turnover on the time scale of the CV. This shows that the catalyst release after the second oxidation is much slower than the formation of intermediates $6f^{OMe}/6f^H$. Accordingly, at least two chemical follow-up steps must follow the oxidation of $6f^{OMe}/6f^H$ in MeCN: a very fast one accounting for the irreversibility of the oxidation process of $6f^{OMe}/6f^H$ and a slower second one forming the 3-pyrroline $4f$ and releasing the catalyst. In line with this CV analysis, i) the current decreased steadily within the first 45 min in the CPE experiment of substrate $1f$ and selenide 3^{OMe} and remains constant afterwards (Figure S1), and ii) product $4f$ is only formed after all catalyst 3^H is consumed in the photochemical experiment (*vide infra*).

In fluorobenzene, the oxidation of the selenide intermediate $6f^{OMe}$ occurs at a peak potential of $E_p = 0.94$ V ($\nu = 0.2$ Vs^{-1}), but the oxidation exhibited a slight reversibility indicating that $6f^{OMe+}$ is more stable in this nonpolar solvent (Figure 1). Analysis of the scan rate dependent CV measurements of $6f^{OMe}$ in fluorobenzene allowed to estimate the half-life τ of the cation $6f^{OMe+}$ with 0.34 s at 25 °C (Figure S8). To determine the reaction order of $6f^{OMe+}$ in the follow-up reaction, concentration dependent CV measurements were conducted, but the analysis was not conclusive, as the experimental error was too large. However, digital simulation of the scan rate dependent data over a large scan rate range applying a Butler-Volmer model suggests a bimolecular rather than a unimolecular follow-up reaction, because the current decrease of the reduction process is too pronounced in the simulation when assuming a unimolecular reaction (Figure 1, Figure S14, S15, further details on the simulation in the SI). The simulation revealed a redox potential of $E^0 = 0.905$ V for $6f^{OMe+}|6f^{OMe}$ and a second order rate constant k_{chem} of about 2.2×10^3 M^{-1}·s^{-1} (corresponding to a half-life τ_{sim} of 0.23 s) for the follow-up reaction in fluorobenzene. A second order reactivity was also previously observed during the oxidation of β-selenenylated lactones in MeCN, which, according to our proposal, resulted in the formation of dimeric dications (i.e., analogous to $[6f^{OMe}]_2^{2+}$).[13]

CV measurements of the intermediate $6f^H$ in fluorobenzene revealed that its oxidation potential is slightly higher than that of $6f^{OMe}$ ($E_{ip/2} = 1.24$ V, $\nu = 0.2$ Vs^{-1}), due to the electron-donating character of the methoxy groups (Figure S9, S11). Notably, the oxidation potentials of the catalyst 3^H and the selenide intermediate $6f^H$ are both lower than the excited state reduction potential of 2^{*BF4} (1.35 V vs. Fc$^{+|0}$ in MeCN).[22] Indeed, Stern-Volmer analyses of compounds 3^H and $6f^H$ led to fluorescence quenching constants K_{SV} of $(2.0 \pm 0.3) \times 10^2$ M^{-1} and $(5.6 \pm 1.7) \times 10^1$ M^{-1}, respectively, that is, the catalyst 3^H is oxidized about 4 times faster by 2^{*BF4} than the intermediate $6f^H$ (Figure S29). Facile formation of the intermediate $6f^H$ as initial step also under photochemical conditions was further confirmed by time-dependent NMR studies. When the product formation of an irradiated ($\lambda = 465$ nm) mixture of catalyst 3^H, substrate $1f$, additive 5^{Cl}, and photocatalyst 2^{BF4} was monitored over the course of 130 min, an initiation phase of 20 min was observed and then the yield of the product $4f$ began to rise almost linearly throughout the following 80 min (Figure 2). This supports that oxidation of the diselenide 3^H and subsequent formation of the intermediate $6f^H$ is fast, whereas the second sequence leading to the product $4f$ is much slower. Indeed, there is no lack phase in the formation of the product $4f$ when intermediate $6f^H$, substrate $1e$, selenide catalyst 3^H, disulfide 5^{Cl}, and pyrylium salt 2^{BF4} are irradiated (Figure 2, yellow curve). In addition, the initial rate for the conversion of the intermediate $6f^H$ to 3-pyrroline $4f$ (dotted yellow line) is similar to the rate of the conversion of the alkene $1f$ into the product $4f$ in the presence of 2^{BF4}, 3^H, and 5^{Cl} after the initiation phase (dotted red line), thus confirming that the selenide $6f^H$ is indeed the kinetically relevant intermediate in the proposed cycle.[23]

Since the initial reaction sequence from the alkene $1f$ to the intermediate $6f^{H/OMe}$ is fast under both, photo- and electro-
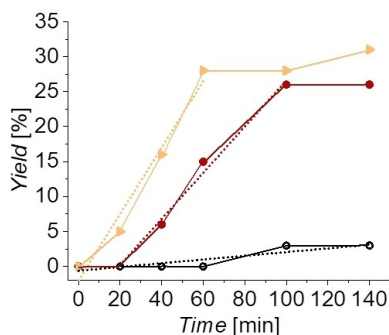
ChemSusChem

Research Article
doi.org/10.1002/cssc.202301518

Chemistry
Europe
European Chemical
Societies Publishing

Figure 2. Yield of **4f** starting from **1f** in the presence of the diselenide catalyst **3**[H] (10 mol%) and the photocatalyst **2**[BF4] (5 mol%) (black curve). Yield of the product **4f** starting from **1f** in the presence of **3**[H] (10 mol%), **5**[Cl] (10 mol%), and **2**[BF4] (5 mol%) (red curve). Yield of **4f** starting from the intermediate **6f**[H] in the presence of **5**[Cl] (10 mol%), **2**[BF4] (5 mol%), and **1e** (100 mol%) (yellow curve). Yields were determined by ^{1}H-NMR spectroscopy using 1,3,5-trimethoxybenzene as an internal standard.

chemical, conditions, we focused next on the impact of the disulfide additive **5**[Cl] on the second half of the reaction cycle from the intermediate **6** to the product **4** (Scheme 3). Irradiation of a mixture of alkene **1f**, disulfide additive **5**[Cl], diselenide catalysts **3**[H], and photocatalyst **2**[BF4] (Figure 2, red curve) furnishes the product **4f** much faster than in the absence of the disulfide **5**[Cl] (Figure 2, black curve), confirming that the co-catalyst **5**[Cl] indeed accelerates the product formation.

Therefore, we had a closer look on the redox properties of disulfide **5**[Cl] to elucidate its role in the protocol. The CV data of disulfide **5**[Cl] in MeCN showed an irreversible oxidation at $E_p = 1.26$ V ($v = 0.2$ Vs^{-1}), which shifts with increasing scan rates and remains irreversible over the whole scan rate range up to 2 Vs^{-1} (Figure S17). In fluorobenzene, however, the oxidation of **5**[Cl] at $E_p = 1.32$ V is reversible at scan rates above ~ 0.2 Vs^{-1} (Figure 3, Figure S17). This observation implies that the follow-up reaction of **5**[Cl+] is slower in the less polar solvent fluorobenzene than in MeCN, as is true for intermediate **6f**[OMe+]. The redox process of **5**[Cl] is a one-electron oxidation, as determined from the scan rate dependent measurements by using the Randles-Ševčík equation (Figure S18). Digital simulation of the CV data of disulfide **5**[Cl] indicates a second order reactivity in **5**[Cl+] as a follow-up reaction (Figures S19, S20). The current of the reduction of radical cation **5**[Cl+] is slightly more overestimated at high scan

rates and underestimated at low scan rates in case of modelling a first order follow-up reaction (Figure S20). The simulation reveals a redox potential of $E^0 = 1.275$ V for **5**[Cl+]|**5**[Cl] and a second order rate constant k_{chem} of about 2.5×10^2 M$^{-1} \cdot$s^{-1} (corresponding to a half-life τ_{sim} of 1.4 s) for the follow-up reaction – e.g. formation of a tetrameric sulfur dication [(**5**[Cl]-**5**[Cl])$_2$]$^{2+}$ similar to what has been proposed previously for diselenide radical cation **3**[H+].[13] There is precedent in the literature for related tetrameric chalcogen dications [R$_4$Ch$_4$]$^{2+}$ (Ch = Se, Te, R = Me, Et, albeit not for Ch = S),[24] which are proposed to result from dimerization of [R$_2$Ch$_2$]$^+$. [R$_4$Ch$_4$]$^{2+}$ is reported as being aromatic in nature, which may represent a possible driving force for dimerization despite electrostatic repulsion.[24]

The oxidation potential of the co-catalyst **5**[Cl] is *higher* than the applied potential during electrocatalysis, and thus its corresponding radical cation is not formed under these conditions. However, it is lower than the excited state reduction potential of photocatalyst **2**[*BF4]. In line with the electrochemical results, fluorescence quenching experiments of the photocatalyst **2**[BF4] and disulfide **5**[Cl] revealed that the latter is oxidized by **2**[*BF4] with a quenching constant K_{SV} of $(1.1 \pm 0.2) \times 10^2$ M^{-1}, which is higher than the quenching rate constant of the selenide intermediate **6f**[H] but lower than that of the diselenide catalyst **3**[H] (Figure S29).

Since **5**[Cl] is oxidized by the photoredox catalyst **2**[*BF4] under photochemical conditions forming **5**[Cl+], we surmised that this could react - in analogy to the proposed reactivity for diselenide radical cation **3**[OMe+] - with alkene **1f** to furnish the analogous sulfide intermediate **7f**[Cl], which upon further oxidation furnishes the product **4f** (Scheme 4). To gain further insight into this potential scenario, **7f**[Cl] was synthesized by alternative means and electrochemically characterized in MeCN and fluorobenzene (Figure S21). Oxidation of **7f**[Cl] occurs at a higher potential ($E_p = 1.39$ V vs. Fc$^{+|0}$ at 0.2 Vs^{-1} in fluorobenzene) than that of the photocatalyst **2**[*BF4], thus making an SET from the former to the latter endergonic. In line with this electrochemical result, no product formation was observed upon irradiating a mixture of intermediate **7f**[Cl], photocatalyst **2**[BF4], and **3**[H], corroborating that the formation of putative intermediate **7f**[Cl] is not a viable route for formation of the product **4f** under photochemical conditions.
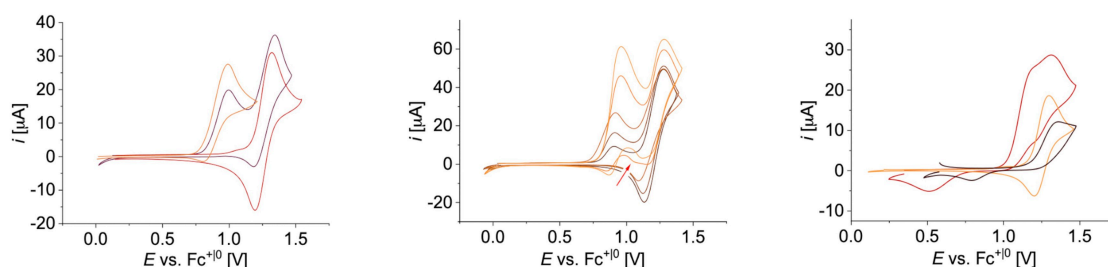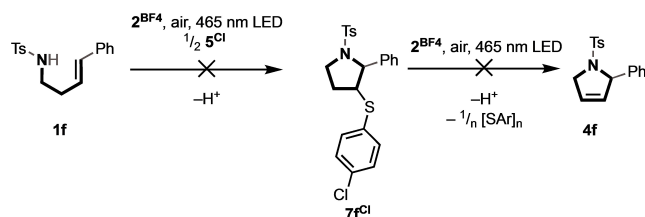

Figure 3. Left: CV measurements of intermediate **6f**[OMe] (orange), $c_{6fOMe} = 4$ mM, disulfide **5**[Cl] (red), $c_{5Cl} = 4$ mM, and a mixture of **6f**[OMe] and **5**[Cl] (dark brown), scan rate $v = 0.2$ Vs^{-1}. Middle: CV measurements of disulfide **5**[Cl], with various amounts of intermediate **6f**[OMe], $c_{6fOMe} = 1, 2, 4, 6, 8$ mM, $c_{5Cl} = 4$ mM, scan rate $v = 0.4$ Vs^{-1}. Right: CV of **5**[Cl] (orange), $c_{5Cl} = 4$ mM, **8**[PF6] (black), $c_{8PF6} = 6$ mM, and a mixture of **5**[Cl] and **8**[PF6] (red), scan rate $v = 0.05$ Vs^{-1}. All data in fluorobenzene with 0.1 M ^{n}Bu$_4$NB(C$_6$F$_5$)$_4$.

ChemSusChem

Research Article
doi.org/10.1002/cssc.202301518

**Chemistry Europe**
European Chemical
Societies Publishing

Scheme 4. Proposed photoredox catalysis utilizing 5^{Cl} as catalyst that was excluded.

Since the sulfur radical cation 5^{Cl+} was found to be considerably stable in nonpolar solvents such as fluorobenzene, and exhibits a higher oxidation potential than that of the diselenide catalyst 3^H as well as the intermediate $6f^H$, we surmised that it may serve as an electron hole reservoir in the photochemical protocol. That is, 5^{Cl} is oxidized by photoexcited 2^{+BF4} and subsequently, undergoes a homogeneous electron transfer reaction with 3^H or $6f^H$ forming the oxidized species. To substantiate this hypothesis, CV experiments with mixtures of intermediate $6f^{OMe}$ and disulfide 5^{Cl} in various ratios were pursued. Addition of disulfide 5^{Cl} (0.25 equiv. to 2 equiv.) had no impact on the half-life of the intermediate $6f^{OMe+}$ (Figure S23): The currents of the oxidation and reduction process in the CV data of intermediate $6f^{OMe}$ were not altered upon adding 5^{Cl}, when the potential is reversed *below* the oxidation potential of 5^{Cl} (i.e., ≤ 1.15 V). This observation is in line with the CPE experiments, in which 5^{Cl} had no effect on the yields. However, when the potential was reversed beyond the oxidation potential of 5^{Cl}, *both* oxidation events become irreversible already at low scan rates, indicating a reduced half-life of both oxidized intermediates, radical cation $6f^{OMe+}$ and disulfide radical cation 5^{Cl+} (Figure 3, Figure S24). The lower reductive current for $6f^{OMe+}$ and for 5^{Cl+} once they co-exist indicates that 5^{Cl+} and $6f^{OMe}$ are not just undergoing a homogeneous electron transfer reaction but are engaged in a chemical follow-up reaction. This fact was supported by the observation that the reduction feature of the intermediate $6f^{OMe+}$ decreases with increasing amounts of disulfide 5^{Cl+}, suggesting the consumption of intermediate radical cation $6f^{OMe+}$ by 5^{Cl+} (Figure 3, middle, Figure S24). Notably, a new reduction feature appears in these titration experiments in the cathodic scan at $E_p = 1.08$ V at a scan rate of 0.4 Vs^{-1}. This is in between the reduction potentials of the intermediate $6f^{OMe+}$ ($E_p = 0.89$ V) and disulfide radical ion 5^{Cl+} ($E_p = 1.20$ V; $\nu = 0.4$ Vs^{-1}), which points to the formation of an interchalcogen species. To collect further evidence for the formation of an interchalcogen dication as a viable intermediate, we investigated the redox behavior of *in-situ* formed PhSePF$_6$, 8^{PF6}, in the absence and presence of 5^{Cl}. 8^{PF6} was synthesized as previously reported[13] by adding AgPF$_6$ to PhSeBr and filtration of the solution. 8^+ exhibits an irreversible oxidation feature in fluorobenzene at $E_p = 1.37$ V and a corresponding reduction feature at $E_p = 0.76$ V ($\nu = 0.1$ Vs^{-1}, Figure S26). Addition of the disulfide 5^{Cl} to a solution of 8^+ leads to a new oxidation process at a *lower* potential than that of 8^+ ($E_p = 1.20$ V) and 5^{Cl}, pointing to the formation of a mixed selenium-disulfur-species that is oxidized more easily

than 8^+ and 5^{Cl} (Figure 3, right, Figure S27). A second irreversible oxidation feature appears at low scan rates of 0.1 Vs^{-1} at $E_p = 1.31$ V. Furthermore, the reversibility of the redox process of $5^{Cl}|5^{Cl+}$ is fully lost in the presence of 8^+, and the reduction feature of the latter disappeared, which substantiates the formation of dicationic interchalcogen species under such oxidative conditions.

Taking all measurements together, we propose the following mechanism for the multicatalytic formation of 3-pyrroline $4f$ (Scheme 5). The photo-excited catalyst 2^{*BF4} and likely disulfide cation 5^{Cl+}, which is formed *in-situ* in a second photoredox cycle *via* oxidation of 5^{Cl} by 2^{*BF4}, serve as one-electron oxidants for 3^H and $6f$. Although, SV plots indicate that diselenide 3^H is oxidized more efficiently by 2^{*BF4} than 5^{Cl}, the kinetic trace shows that 3^H is fully consumed forming the intermediate $6f$ prior to product formation. That means that the concentration of 3^H is very small under steady state conditions and thus, the reaction rate for oxidation of disulfide 5^{Cl} by 2^{*BF4} should become competitive. Further, oxidation of 5^{Cl} by 2^{*BF4} is more efficient than of $6f^H$ and thus, 5^{Cl} could be an important primary electron donor under steady-state conditions. The $5^{Cl}|5^{Cl+}$ couple has an oxidation potential E^0 of 1.275 V in fluorobenzene, which is higher than the one of diselenide 3^H and $6f^H$, and 5^{Cl+} exhibits a considerably long lifetime in fluorobenzene and thus could serve as electron hole reservoir in non-polar solvents. Direct oxidation of the tosylamides 1 by photo-excited 2^{*BF4} is not feasible as alkyl tosylamides exhibit oxidation potentials >2 V vs. Fc$^{+|0}$, which is higher than the redox potential of 2^{*BF4}.[27]

Oxidation of 3^H provides access to radical cation 3^{H+}, which reacts with alkene $1f$ to furnish intermediate $6f^H$. Oxidation of the intermediate $6f^H$ by 2^{*BF4} or 5^{Cl+} provides access to the radical cation $6f^{H+}$. Under photoredox catalytic conditions, we assume that $6f^{H+}$ is intercepted by 5^{Cl+} to give an interchalcogen dication $[6f^H-5^{Cl}]^{2+}$ based on the observed reduction of the half-lives of $6f^{OMe+}$ and 5^{Cl+} once they co-exist. Product $4f$ is eliminated from this interchalcogen dication, yielding the
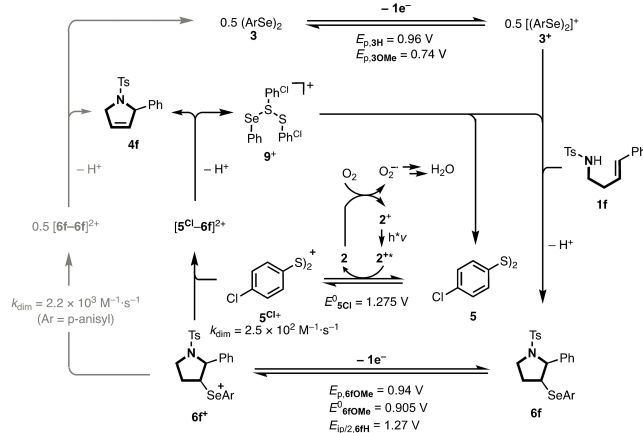
Scheme 5. Proposed catalytic cycle for the aza-Wacker cyclization of alkene $1f$, catalyzed by the diselenide 3^H under photo-aerobic conditions. The grey pathways refer to the pathway under electrochemical conditions. Potentials and reaction rate constants are given for fluorobenzene; (half) peak potentials are given for $\nu = 0.2$ Vs^{-1}; fluorobenzene.

ChemSusChem

Research Article
doi.org/10.1002/cssc.202301518

Chemistry Europe
European Chemical
Societies Publishing

adduct 9^+ $[(o\text{-anisyl})Se-S(C_6H_4\text{-}p\text{-Cl})-S(C_6H_4\text{-}p\text{-Cl})]^+$ and H^+. Homologous trimeric chalcogen cations have precedents in the literature, and are structurally well characterized, *cf.* $[Me_3S_3]^+$, $[Me_3Se_3]^+$, $[(C_6F_5S)_3]^+$.[25] The cationic interchalcogen adduct 9^+ likely transfers its remaining selenenium residue directly onto a second equiv. of the alkene **1f** forming **6f**^{H} again. However, we cannot exclude an equilibrium of 9^+ with dissociated $PhSe^+$ and disulfide **5**^{Cl}, which would also close the catalytic cycle. The considerable longevity of radical cation **5**$^{Cl+}$ in fluorobenzene compared to that in MeCN could explain the benign impact of nonpolar solvents (e.g., *o*-xylene) on the photoredox catalytic process, despite the lower solubility of photocatalyst **2**^{BF4} therein. Running electrolysis at potentials sufficient to oxidize the disulfide **5**^{Cl}, however, leads to electrode fouling, and therefore the use of **5**^{Cl} in an electrocatalytic regime is not a feasible approach.

Conclusions

In summary, we have developed a selenium-π-acid catalyzed aza-Wacker cyclization of unsaturated sulfonamides, which, for the first time, was found to be suitable for the synthesis of 3-pyrrolines. The title procedure is operationally simple, tolerant of various functional groups, and furnishes the products in up to 99% yield. Advanced electrochemical mechanistic investigations revealed that the reaction proceeds through a sequence of electrophilic addition and elimination reaction, in which the (di)selane catalyst is undergoing photo-aerobic one-electron-oxidation forming the selenium cation. Consequently, the substrates are converted in an ionic regime, even though the individual oxidation steps are one-electron steps.[26] We have strong evidence from electrochemical measurements for the participation of the disulfane cation **5**$^{Cl+}$ under photoredox catalytic conditions through the transient formation of dicationic interchalcogen species that accelerate the release of the aza-Wacker products from the intermediate **6f**$^{H+}$. This novel form of photo-aerobic interchalcogen catalysis appears very promising for the design of other redox functionalizations of alkenes, in particular with regard to enantioselective transformations, and therefore lay the fundament for future activities in this direction in our laboratories.

Experimental section

General remarks

All reagents for chemical synthesis were purchased from commercial sources and were used without further purification. Solvents were used in p.a. quality or dried by storage over molecular sieves under N_2 atmosphere. Irradiation experiments for the intermolecular amination reaction were performed at $\lambda = 465$ nm using commercially available blue LED strips. The light intensity applied was in the range of 4300-4800 lx. Custom built temperature-controlled metal blocks for light irradiation were used (15000-17000 lx). All reagents for electrochemical measurements were purchased as electrochemical or HPLC grade. MeCN was purified over the *Solvent Purification System* from *MBraun* and stored over

molecular sieve (3 Å) before use. Fluorobenzene was dried over P_2O_5 and stored over molecular sieve (3 Å) before use. Electrochemical grade $^nBu_4NPF_6$ was purchased from *Sigma-Aldrich* and dried at 244 °C under high vacuum prior to use. $^nBu_4NB(C_6F_5)_4$ was synthesized according to literature procedures.[28] Electrochemical CV measurements were carried out in a custom-made three-neck glass cell using a *Gamry Instruments Reference [600]* or a *1010B* in anhydrous MeCN or fluorobenzene under air, except those of **8**^{PF6} and **8**^{Br}, which were done in an MBraun glovebox operated under N_2 atmosphere with dry and degassed solvents. A common three electrode setup was used with a glassy carbon working electrode (MeCN: *CH Instruments, ALS Japan*; A = 7.1 mm^2, fluorobenzene: *CH Instruments, ALS Japan*; A = 2.0 mm^2), a platinum wire as a counter electrode, and a silver wire in silver nitrate solution ($c = 0.01$ M) in the case of MeCN, and just a silver wire in the case of fluorobenzene. $^nBu_4NPF_6$ was used as conducting salt for MeCN ($c = 0.1$ M) and $^nBu_4NB(C_6F_5)_4$ ($c = 0.1$ M) for fluorobenzene. All data were referenced internally vs. the $Fc^{+|0}$ redox potential, which was added at the end of each measurement.

General procedure for the photo redox reactions: To a solution of the sulfonylaminde **1** (1.00 eq.) in *o*-xylene (0.2 M) **3**^{H} (0.10 eq.) and **2**^{BF4} (0.05 eq.) were added in a 250 mL round bottom flask. The suspension was subjected to irradiation at 465 nm and stirred vigorously with a cross shaped stirring bar (750 rpm) at ambient air for the given time. If indicated, **5**^{Cl} (0.10 eq.) or 2-nitrobenzaldehyde (0.25 eq.) were added to the suspension right away or **3**^{H} (0.10 eq.) and **2**^{BF4} (0.05 eq.) were re-added after the indicated time. The solvent was evaporated under reduced pressure and the crude product was purified via column chromatography. For the NMR yield determination, the solvent of the reaction mixture was evaporated under reduced pressure, the residue was dissolved in $CDCl_3$ (0.6 mL) and 1,3,5-trimethoxybenzene (TMB) was added as an internal standard.

General procedure for the electrolysis experiments: A glassy carbon rod ($d = 3$ mm) was used as a working electrode and a curled platinum wire as a counter electrode. An $Ag/AgNO_3$ ($c_{AgNO3} = 0.01$ M in MeCN) electrode served as a reference electrode. The yields were determined by ^1H-NMR spectroscopy with 1,3,5-trimethoxybenzene as internal standard. Therefore, the solvent was removed after electrolysis, the internal standard was added, and the residue was dissolved in CD_2Cl_2. The CCE experiments ($I = 400$ µA) of **3**^{OMe} (1.3 mg, 0.0034 mmol, 1.7 mM) with **1f** (10 mg, 0.033 mmol, 17 mM) in fluorobenzene (2 mL) with $^nBu_4NB(C_6F_5)_4$ (368 mg, 0.2 M) were performed with and without **5**^{Cl} (1.0 mg, 0.0034 mmol, 1.7 mM) giving **4f** with a yield of 35% and 33% (^1H-NMR spectroscopy), respectively. The constant potential electrolysis (CPE) experiments were performed at the potential of 1.15 V vs. $Ag/AgNO_3$ ($c = 0.01$ M in MeCN) with the alkene (0.1 mmol, 33 mM) and **3**^{OMe} in acetonitrile (3 mL) and $^nBu_4PF_6$ (116 mg, 0.1 M) as conducting salt.

Supporting Information

The Supporting Information contains additional detailed experimental procedures, spectroscopic characterization, and additional analytical data. The authors have cited additional references within the Supporting Information.[28–36]

Acknowledgements

ChemSusChem

Research Article
doi.org/10.1002/cssc.202301518

Chemistry Europe
European Chemical
Societies Publishing

Conflict of Interests

The authors declare no conflict of interest.

Data Availability Statement

The data that support the findings of this study are available in the supplementary material of this article.

[1] a) P. M. Dewick, *Medicinal Natural Products*, John Wiley & Sons, Chichester, **2009**; b) C. T. Walsh, *Tetrahedron Lett.* **2015**, *56*, 3075–3081; c) E. Vitaku, D. T. Smith, J. T. Njardarson, *J. Med. Chem.* **2014**, *57*, 10257–10274.

[2] J. E. Redford, R. I. McDonald, M. L. Rigsby, J. D. Wiensch, S. S. Stahl, *Org. Lett.* **2012**, *14*, 1242–1245.

[3] I. R. Hazelden, R. C. Carmona, T. Langer, P. G. Pringle, J. F. Bower, *Angew. Chem. Int. Ed.* **2018**, *57*, 5124–5128.

[4] A. A. Thomas, S. Nagamalla, S. Sathyamoorthi, *Chem. Sci.* **2020**, *11*, 8073–8088.

[5] For an isolated example involving the cyclization of unsaturated carboxamides to give pyrrolones, see: G. B. Bajracharya, P. S. Koranne, R. N. Nadaf, R. K. M. Gabr, K. Takenaka, S. Takizawa, H. Sasai, *ChemComm* **2010**, *46*, 9064–9066.

[6] a) C.-L. J. Wang, J. C. Calabrese, *J. Org. Chem.* **1991**, *56*, 4341–4343; b) M. Kimura, H. Harayama, S. Tanaka, Y. Tamaru, *J. Chem. Soc., Chem. Commun.* **1994**, 2531–2533; c) M. Brichacek, M. Navarro Villalobos, A. Plichta, J. T. Njardarson, *Org. Lett.* **2011**, *13*, 1110–1113; d) N. S. Medran, A. La-Venia, S. A. Testero, *RSC Adv.* **2019**, *9*, 6804–6844.

[7] a) M. B. Tait, S. Butterworth, J. Clayden, *Org. Lett.* **2015**, *17*, 1236–1239; b) A. Perfetto, C. Costabile, P. Longo, V. Bertolasi, F. Grisi, *Chem. Eur. J.* **2013**, *19*, 10492–10496; c) A. Bunrit, S. Sawadjoon, S. Tsupova, P. J. R. Sjoberg, J. S. M. Samec, *J. Org. Chem.* **2016**, *81*, 1450–1460.

[8] a) Q. Wu, J. Hu, X. Ren, J. Zhou, *Chem. Eur. J.* **2011**, *17*, 11553–11558; b) F. F. Tang, W. L. Yang, X. X. Yu, W. P. Deng, *Catal. Sci. Technol.* **2015**, *5*, 3568–3575.

[9] a) M. O. Amombo, A. Hausherr, H.-U. Reissig, *Synlett* **1999**, 1871–1874; b) R. K. Dieter, N. Chen, H. Yu, L. E. Nice, V. K. Gore, *J. Org. Chem.* **2005**, *70*, 2109–2119; c) R. K. Dieter, N. Chen, V. K. Gore, *J. Org. Chem.* **2006**, *71*, 8755–8760; d) B. Mitasev, K. M. Brummond, *Synlett* **2006**, 3100–3104; e) W. Rao, P. Kothandaraman, C. B. Koh, P. W. H. Chan, *Adv. Synth. Catal.* **2010**, *352*, 2521–2530; f) M. Sai, S. Matsubara, *Org. Lett.* **2011**, *13*, 4676–4679; g) J. Brioche, C. Meyer, J. Cossy, *Org. Lett.* **2013**, *15*, 1626–1629; h) R. R. Tata, C. Fu, S. P. Kelley, M. Harmata, *Org. Lett.* **2018**, *20*, 5723–5726; i) S. S. K. Boominathan, W. P. Hu, G. C. Senadi, J. J. Wang, *Adv. Synth. Catal.* **2013**, *355*, 3570–3574; j) A. Hausherr, H.-U. Reissig, *Eur. J. Org. Chem.* **2018**, 4071–4080.

[10] J. E. M. N. Klein, K. Geoghegan, N. Méral, P. Evans, *Chem. Commun.* **2010**, *46*, 937–939.

[11] For representative reviews on this topic, see: a) V. Kotov, C. C. Scarborough, S. S. Stahl, *Inorg. Chem.* **2007**, *46*, 1910–1923; b) R. I. McDonald, G. Liu, S. S. Stahl, *Chem. Rev.* **2011**, *111*, 2981–3019.

[12] a) X. Yi, X. Hu, *Angew. Chem. Int. Ed.* **2019**, *58*, 4700–4704; b) C.-Y. Cai, Z.-J. Wu, J.-Y. Liu, M. Chen, J. Song, H.-C. Xu, *Nature Commun.* **2021**, *12*, 3745; c) C. Huang, Z.-Y. Li, J. Song, H.-C. Xu, *Angew. Chem. Int. Ed.* **2021**, *133*, 11337–11341.

[13] M. Wilken, S. Ortgies, A. Breder, I. Siewert, *ACS Catal.* **2018**, *8*, 10901–10912.

[14] D. J. C. Constable, A. D. Curzons, V. L. Cunningham, *Green Chem.* **2002**, *4*, 521–527.

[15] B. M. Trost, *Science* **1991**, *254*, 1471–1477.

[16] a) V. Kotov, C. C. Scarborough, S. S. Stahl, *Inorg. Chem.* **2007**, *46*, 1910–1923; b) A. A. Thomas, S. Nagamalla, S. Sathyamoorthi, *Chem. Sci.* **2020**, *11*, 8073–8088; c) A. Minatti, K. Muñiz, *Chem. Soc. Rev.* **2007**, *36*, 1142–1152.

[17] S. Ortgies, A. Breder, *ACS Catal.* **2017**, *7*, 5828–5840.

[18] a) J. Trenner, C. Depken, T. J. Weber, A. Breder, *Angew. Chem. Int. Ed.* **2013**, *52*, 8952–8956; b) S. Ortgies, A. Breder, *Org. Lett.* **2015**, *17*, 2748–2751; c) R. Guo, J. Huang, H. Huang, X. Zhao, *Org. Lett.* **2016**, *18*, 504–507; d) L. Liao, R. Guo, X. Zhao, *Angew. Chem. Int. Ed.* **2017**, *56*, 3201–3205; e) Y. Zhang, Y. Shao, J. Gong, T. Cheng, J. Chen, *J. Org. Chem.* **2019**, *84*, 2798–2807; f) H. Li, L. Liao, X. Zhao, *Synlett* **2019**, *30*, 1688–1692; g) X. Wang, Q. Wang, Y. Xue, K. Sun, L. Wu, B. Zhang, *Chem. Commun.* **2020**, *56*, 4436–4439; h) D. C. Obenschain, J. R. Tabor, F. E. Michael, *ACS Catal.* **2023**, *13*, 4369–4375.

[19] S. Ortgies, R. Rieger, K. Rode, K. Koszinowski, J. Kind, C. M. Thiele, J. Rehbein, A. Breder, *ACS Catal.* **2017**, *7*, 7578–7586.

[20] T. Lei, S. Graf, C. Schöll, F. Krätzschmar, B. Gregori, T. Appleson, A. Breder, *ACS Catal.* **2023**, *13*, 16240–16248. .

[21] Table of Dielectric Constants of Pure Liquids, National Bureau of Standards, NBS Circular 514. Date Issued **1951**.

[22] F. Chemla, A. Pérez-Luna, *Science of Synthesis, Free Radicals: Fundamentals and Applications in Organic Synthesis 2 (Eds. L. Fensterbank, C. Ollivier)*, Georg Thieme Verlag KG, **2021**.

[23] a) M. Martiny, E. Steckhan, T. Esch, *Chem. Ber.* **1993**, *126*, 1671–1682. In this reference, the reduction potential of excited **2^BF4*** was reported as 1.98 V vs. NHE. For a direct comparison, we have converted the reduction potential to 1.35 V vs. Fc$^{+|0}$ according to; b) V. V. Pavlishchuk, W. W. Addison, *Inorg. Chim. Acta* **2000**, *298*, 97–102.

[24] We added one equivalent of **1e** to this mixture as a sacrificial reagent to intercept **3^H**, which is released in situ from **6f^H** and would have quenched the photoredox catalyst if not captured by the sacrificial alkene.

[25] a) B. Mueller, H. Poleschner, K. Seppelt, *Dalton Trans.* **2008**, 4424–4427; b) H. Poleschner, K. Seppelt, *Angew. Chem. Int. Ed.* **2013**, *52*, 12838–12842.

[26] a) R. Laitinen, R. Steudel, R. Weiss, *J. Chem. Soc., Dalton Trans.* **1986**, 1095–1100; b) S. Brownridge, T. S. Cameron, J. Passmore, G. Schatte, G. W. Sutherland, *Can. J. Chem.* **1998**, *76*, 1050–1059.

[27] T. Shono, Y. Matsumura, K. Tsubata, K. Uchida, T. Kanazawa, K. Tsuda, *J. Org. Chem.* **1984**, *49*, 3711–3716.

[28] J. L. LeSuer, C. Buttolph, W. E. Geiger, *Anal. Chem.* **2004**, *76*, 6395–6401.

[29] B. A. Gellert, N. Kahlcke, M. Feurer, S. Roth, *Chem. Eur. J.* **2011**, *17*, 12203–12209.

[30] I. R. Hazelden, X. Ma, T. Langer, J. F. Bower, *Angew. Chem. Int. Ed.* **2016**, *55*, 11198–11202.

[31] G. Liu, S. S. Stahl, *J. Am. Chem. Soc.* **2007**, *129*, 6328–6335.

[32] K. Rode, M. Palomba, S. Ortgies, R. Rieger, A. Breder, *Synthesis* **2018**, *50*, 3875–3885.

[33] M. Millard, J. D. Gallagher, B. Z. Olenyuk, N. Neamati, *J. Med. Chem.* **2013**, *56*, 9170–9179.

[34] R. An, L. Liao, X. Liu, S. Song, X. Zhao, *Org. Chem. Front.* **2018**, *5*, 3557–3561.

[35] D. P. Hickey, C. Sandford, Z. Rhodes, T. Gensch, L. R. Fries, M. S. Sigman, S. D. Minteer, *J. Am. Chem. Soc.* **2019**, *141*, 1382–1392.

[36] L. Polleux, E. Labbé, O. Buriez, J. Périchon, *Chem. Eur. J.* **2005**, *11*, 4678–4686.